

SCIENTIFIC REPORTS



OPEN

Enhancement and suppression of turbulence by energetic-particle-driven geodesic acoustic modes

M. Sasaki^{1,2}, K. Itoh^{2,3}, K. Hallatschek^{2,4}, N. Kasuya^{1,2}, M. Lesur⁵, Y. Kosuga^{1,2} & S.-I. Itoh^{1,2}

We propose a novel mechanism of enhancement of turbulence by energetic-particle-driven geodesic acoustic modes (EGAMs). The dynamics of drift-wave-type turbulence in the phase space is investigated by wave-kinetic equation. Spatially inhomogeneous turbulence in the presence of a transport barrier is considered. We discovered that trapping of turbulence clumps by the EGAMs is the key parameter that determines either suppress or enhance turbulence. In regions where turbulence is unstable, EGAM suppresses the turbulence. In contrast, in the stable region, EGAM traps clumps of turbulence and carries them across the transport barrier, so that the turbulence can be enhanced. The turbulence trapped by EGAMs can propagate independent of the gradients of density and temperature, which leads to non-Fickian transport. Hence, there appear a new global characteristic velocity, the phase velocity of GAMS, for turbulence dynamics, in addition to the local group velocity and that of the turbulence spreading. With these effect, EGAMs can deteriorate transport barriers and affect turbulence substantially. This manuscript provides a basis to consider whether a coherent wave breaks or strengthen transport barriers.

Problems including interactions between micro-turbulence and coherent waves are ubiquitous in a variety of systems^{1,2}. The coexistence of global-coherent Alfvén wave and micro-turbulence has been observed at the surface of the sun, which could link with the coronal heating problem³. Turbulence in planetary atmospheres generates zonal flows², such as jet stream on the earth, stripes of Jupiter, super rotation on Venus, and tachocline on the sun⁴. In magnetically confined plasmas, geodesic acoustic modes (GAMs), which are oscillatory zonal flows, have attracted much attention as coherent waves, because GAMs are expected to suppress turbulence by their velocity shear¹. Actually, the suppression of turbulence and transport have been reported in turbulence simulations⁵. Experimental study has shown that the transition to high confinement state is accompanied by GAMs⁶. However, recently, the enhancement of turbulence by GAMs has been observed in first principle simulations, with the subsequent destruction of a transport barrier⁷⁻⁹. In this way, GAMs can either mitigate or enhance the turbulence. This dual effect of the GAMs on turbulence requires theoretical investigation.

We investigate the phase-space dynamics of spatially inhomogeneous turbulence in the presence of GAMs. GAMs are driven not only by turbulence^{5,10} but also by energetic particles (EPs), which are called EGAM¹¹⁻¹⁴. Turbulence driven GAMs suppress turbulence, which can be understood in terms of energy conservation (the total energy of GAMs and turbulence is conserved). In contrast, the impacts of EGAMs on turbulence is not clear, in particular because EGAMs obtain their energy from EPs, not from turbulence. Actually, EGAMs have been reported to enhance turbulence in spite of the fact that EGAMs have velocity shears^{7,8}. In order to clarify the impact of finite-frequency zonal flows on turbulence, we focus on EGAMs. The phase-space dynamics results in trapping of turbulence wave-packets by EGAMs¹⁵. We found that the trapped turbulence wave-packets leak across the transport barrier. As a result, turbulence is enhanced by EGAMs in the stable region, while turbulence suppression is obtained in the unstable region. We discovered that trapping of turbulence clumps by the EGAMs is the key parameter that determines either suppress or enhance turbulence. The propagation of the turbulence is ballistic, with the phase velocity of the EGAM. Thus, the turbulence propagation is in some sense independent from the background profiles such as the gradients of density and temperature. Thus, turbulence carried by the

¹Research Institute for Applied Mechanics, Kyushu University, Kasuga, 816-8580, Japan. ²Research Center for Plasma Turbulence, Kyushu University, Kasuga, 816-8580, Japan. ³Institute of Science and Technology Research, Chubu University, Kasugai, 487-8501, Japan. ⁴Max-Planck-Institute for Plasma Physics, 85748, Garching, Germany. ⁵Lorraine University, Institut Jean Lamour, Nancy, 54-506, France. Correspondence and requests for materials should be addressed to M.S. (email: sasaki@riam.kyushu-u.ac.jp)

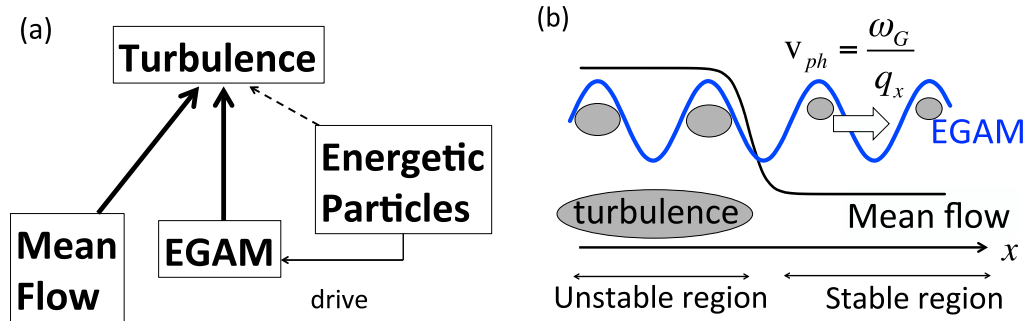


Figure 1. (a) Model on relationship between turbulence, mean flow, EGAM and EPs. (b) Model geometry of the inhomogeneous turbulence with the mean flow.

EGAMs shows non-Fickian transport properties. The propagation of trapped turbulence is different from processes such as turbulence spreading^{16–18}, avalanches^{19–21} and others^{22,23}. Hence, there appear a new global characteristic velocity, the phase velocity of GAMS, for turbulence dynamics, in addition to the local group velocity and that of the turbulence spreading.

Results

Problem setting. We consider the dynamics of spatially inhomogeneous turbulence with a transport barrier in the presence of EGAMs. We focus on the impact of EGAM on turbulence. As the first step, in order to simplify the problem, we neglect the direct effect of EPs on turbulence, as shown in Fig. 1(a). The radial profile of the flux surface averaged turbulence intensity is studied. The radial direction is set to x -direction. We consider a situation where the turbulence unstable region faces the stable region, and a transport barrier is localized at the boundary, as shown in Fig. 1(b). The transport barrier is simulated by a mean sheared flow. Turbulence is set to be linearly unstable (stable) inside (outside) the shear layer, respectively. The EGAM is assumed to have only a positive radial wavenumber, so the EGAM propagates from inward to outward the shear layer. It is noted that the EGAM has several branches; one has almost zero poloidal wavenumber $q_y \approx 0$ ¹¹ and another has a steep poloidal structure²⁴. In this study, we focus on the branch with $q_y \approx 0$, which is unaffected by the doppler-shift due to the mean sheared flow. This branch is driven by the resonance with the toroidally passing EPs, where we neglect the effect of the magnetically trapped EPs. In such a situation, the turbulence is governed by the wave-kinetic equation²⁵,

$$\frac{\partial N_k}{\partial t} + \frac{\partial \omega_k}{\partial k} \cdot \nabla N_k - \nabla \omega_k \cdot \frac{\partial N_k}{\partial k} = \gamma_L N_k - \Delta \omega N_k^2, \quad (1)$$

where N_k and ω_k are the normalized action and frequency of the turbulence, respectively²⁵. The linear growth rate and the nonlinear decorrelation rate of turbulence are denoted by γ_L , and $\Delta \omega$, respectively. Here time and space are normalized by $\rho_s^{-1} V_d$ and ρ_s , where V_d is the diamagnetic drift velocity, and ρ_s is the ion gyro-radius measured by the sound velocity. It is noted that the typical frequency of the turbulence satisfies the relation, $\omega = \rho_s^{-1} V_d \gg \omega_G \sim \omega_{EP}$, where ω_{EP} is the transit frequency of EPs. Thus, we assume that the resonance of the EPs with the turbulence is weaker than that with EGAMs. We treat γ_L as an independent parameter on EPs. We consider drift-wave-type turbulence, so N_k is given as $N_k = (1 + k_x^2 + k_y^2)^2 |\tilde{\phi}_k|^2$, and the frequency ω_k is

$$\omega_k = \frac{k_y}{1 + k_x^2 + k_y^2} + k_y V_y(x, t), \quad (2)$$

where $\tilde{\phi}_k$ is the normalized turbulent electrostatic potential, and k_x, k_y are the turbulence wavenumbers. The turbulence frequency ω_k includes the doppler shift due to $V_y(x, t)$, which consists of the EGAM and the mean flow.

The turbulence trapping in the phase space was investigated in the previous studies^{15,26}. Here, we compare the assumptions and results between these previous studies^{15,26} and the present work. In these studies, an analytic solution for a nonlinear wave pattern for zonal flows was obtained by considering the interaction between turbulence driven zonal flows and turbulence. The following assumptions were used; spatially homogeneous turbulence with a marginal stability condition was assumed ($\gamma_L = \Delta \omega = 0$), and the k_x -spectrum distribution of N_k was prescribed. The dispersion relation for the drift wave in the paper¹⁵ is the same with that in this study, Eq. (2). In this study, prescribing the EGAM evolution, which is valid for the EP driven mode, we consider the spatially inhomogeneous turbulence by introducing the turbulence source ($\gamma_L, \Delta \omega$), and the mean flow shear. We obtain the k_x -spectrum evolutions of N_k without any assumption for the distribution. By considering the spatially inhomogeneous turbulence, we discover that the trapped turbulence clump can penetrate into the stable region with the ballistic propagation, which leads to enhancement of turbulence there.

Trapping of turbulence by EGAM. Let us describe the results obtained from the simulation. Figure 2 illustrates snapshots of N_k in the phase space (x, k_x) , and the time evolution of the turbulence intensity $I(x) = \int (1 + k_x^2)^{-2} N_k d^2 k$ in the real space, where k_\perp is defined as $k_\perp = \sqrt{k_x^2 + k_y^2}$. The boundary between the

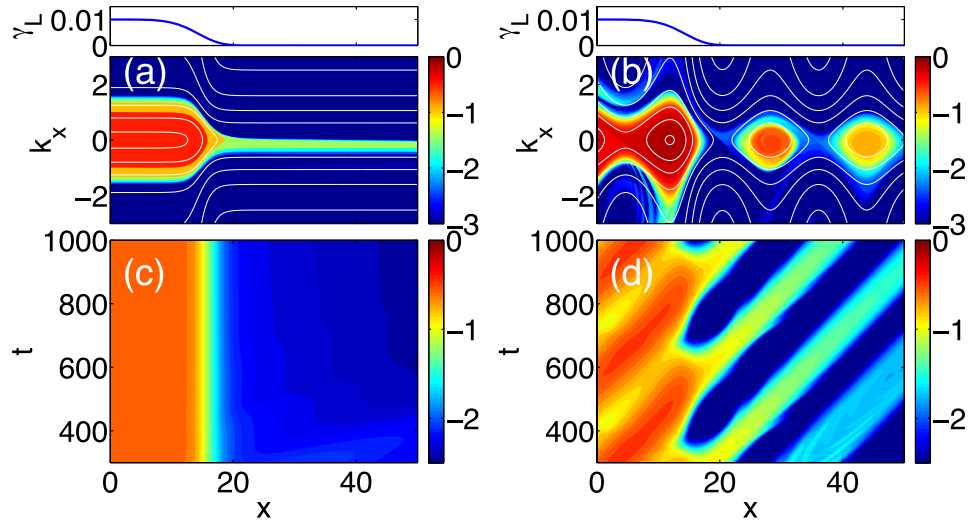


Figure 2. Snap-shots of N_k in the case of (a) $V_G = 0$, and (b) $V_G = 0.1$ at $t = 800$ are shown. The time evolution of turbulence intensity is shown for the case of (c) $V_G = 0$, and (d) $V_G = 0.1$.

turbulence unstable region and the stable region is $x \approx 20$, and the shear layer is localized around the boundary. The results without the EGAM ($V_G = 0$) are shown in Fig. 2(a,c). Here, V_G is the amplitude of the $E \times B$ velocity of the EGAM. The k_x -spectrum of the turbulence in the unstable region $x < 20$ has positive-negative symmetry with respect to k_x . In the stable region, the k_x -spectrum becomes asymmetric, and the turbulence exists only for $k_x < 0$, where the group velocity of the turbulence is positive. This outflow of the turbulence into the stable region can be understood by considering the motion of the quasi-particles (QPs). The equation of motion for the QPs is governed by Eq. (1) is^{15,26}

$$\dot{x}(t) = \frac{\partial \omega_k}{\partial k_x} = -\frac{2k_x(t)k_y}{(1 + k_x(t)^2 + k_y^2)^2}, \quad (3)$$

$$\dot{k}_x(t) = -\frac{\partial \omega_k}{\partial x} = -k_y \frac{\partial V_y(x, t)}{\partial x} \Big|_{x=x(t)}, \quad (4)$$

with $k_y = \text{const}$. Equations (3) and (4) correspond to the characteristics of Eq. (1), in the same way that, for example, the equations of motion of plasma particles correspond to the characteristics of the Vlasov equation. When the amplitude of the EGAM is zero and V_y is stationary, the motion of the QP becomes integrable. The drift frequency which includes the doppler shift due to the mean flow, Eq. (2), becomes a constant of motion. From this constant, the trajectories of the QPs are determined by

$$k_x(x)^2 = \frac{1}{C - V_y(x)} - (1 + k_y^2), \quad (5)$$

where C is a constant parameter, $C = k_y^{-1} \omega_k$. Depending on the initial k_x , the solution becomes bounded in the real space ($|k_x| < k_c = \sqrt{2V_{MF}(1 + k_y^2)(1 - 2V_{MF}(1 + k_y^2))^{-1}}$), which corresponds to trapped motion in the unstable region, or becomes boundless ($|k_x| > k_c$), which corresponds to the transit motion across the shear layer. Here V_{MF} is the magnitude of the mean flow as defined in Eq. (12).

Next, we consider a case with finite amplitude EGAM. The numerical results with $V_G = 0.1$ are shown in Fig. 2(b,d). The turbulence is modulated by the EGAM, temporally and spatially, in the unstable region, $x < 20$. In the stable region $x > 20$ (where there is no turbulence source, and the turbulence is affected by the nonlinear decorrelation), turbulence trapped by the EGAM forms islands in the phase space. As seen from the time evolution of the turbulence intensity in Fig. 2(d), the trapped turbulence propagates with the phase velocity of the EGAM, $v_{ph} = q_x^{-1} \omega_G = 0.05$. The dynamics of the turbulence can be understood by considering the motion of the QPs. When the time variation of the EGAM is negligibly small $\omega_G \ll q_x v_g$, ω_k becomes an adiabatic constant of motion. From Eq. (5), the trajectories of the QPs in the stable region can be categorized as

$$|k_x| < k_{sep} = \sqrt{\frac{(1 + k_y^2)^2 V_G}{1 - (1 + k_y^2) V_G}} : \text{trapped}, \quad (6)$$

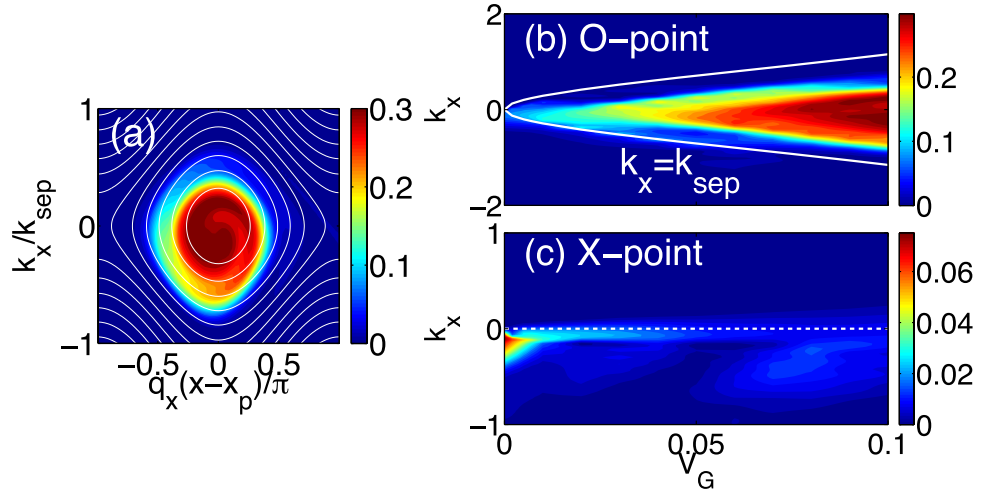


Figure 3. (a) Phase-space structure of the turbulence trapped by the EGAM in the stable region. The white lines are the contours of ω_k . Dependence of k_x -spectrums of the island at (b) O-point and (c) X-point on the amplitude of the EGAM are shown.

$$k_{sep} < |k_x| < k_* = \sqrt{\frac{1 - (1 + k_y^2)V_G}{V_G}}: \text{transit}. \tag{7}$$

When $|k_x| > k_*$, the QPs are reflected by the shear of the EGAM and the wavenumber diverges. The QPs with $k_x < k_{sep}$ are trapped by the EGAM, which results in an island.

The propagation distance of the turbulence in the stable region is derived. The trapped turbulence clump in the stable region at $k_x = 0$ is governed by $\partial_t N_k = -\Delta\omega N_k^2$. The solution of the envelope of the turbulence clump can be obtained as

$$N_k = \frac{1}{\omega_G^{-1}\Delta\omega q_x(x - x_0) + 1/N_{k,0}}. \tag{8}$$

The trapped turbulence decays algebraically (unlike quantum tunneling) in space, with the typical scales, $\omega_G\Delta\omega^{-1}q_x^{-1}$. The decay length derived here is consistent with the simulation results.

We describe two mechanisms by which the turbulence propagates in the stable region; one occurs without the EGAM (transit loss), and another is due to the turbulence trapping by the EGAM (trapped loss). We investigate conditions for trapped loss to be dominant. Figure 3 shows the change of the island shape as V_G varies. The island in the case of $V_G = 0.1$ is shown in Fig. 3(a). Here the island is obtained from the ensemble average of islands, which satisfy $q_x x_p - \omega_G t = (1/2 + n)\pi$ (n is an integer, and $x_p = 27$) with $t < 1000$. The amplitude dependence of the k_x -spectra of ensemble averaged N_k at X-point, $q_x(x - x_p) = \pi$, and at O-point, $q_x(x - x_p) = 0$, are shown in Fig. 3(b,c). With increasing V_G , the intensity of the turbulence increases inside the island $k_x < k_{sep}$. When the EGAM amplitude is small, $V_G < 0.03$, the intensity inside the island is ambiguous, and the turbulence at X-point exists in $k_x < 0$. If the turbulence trapping is perfect, the turbulence does not exist at X-point. Thus, the transit loss is dominant when the amplitude is small. The conditions for the EGAM amplitude that the trapped loss becomes important can be understood as follows. Two conditions are necessary for the trapped turbulence to leak into the stable region. The first condition is that the turbulence is trapped by the EGAM. The trapped turbulence moves within the EGAM island with the bounce frequency $\omega_b = \sqrt{2k_y^2 q_x^2 V_G (1 + k_y^2)^{-2}}$. In order to be trapped by the EGAM, the QPs should have a bounce period shorter than the EGAM period. Thus, the trapping condition is $\omega_G < \omega_b$. This condition can be written as

$$V_G > \frac{\omega_G^2 (1 + k_y^2)^2}{2k_y^2 q_x^2}. \tag{9}$$

For our parameters, this condition is $V_G > 0.005$. When $\omega_b \sim \omega_G$, there is a possibility that the turbulence clump itself directly resonates with EPs. In such a situation, the trapping condition for the turbulence clump, Eq. (9), may be modified qualitatively. However, this effect is beyond the scope of this study, and we neglect it here. The second condition is that the trapped turbulence crosses the transport barrier. In order to leak across the shear layer, the bounce period should be shorter than the transit time of the shear layer $\tau = q_x \Delta \omega_G^{-1}$, where Δ is the width of the shear layer. Thus, the condition is

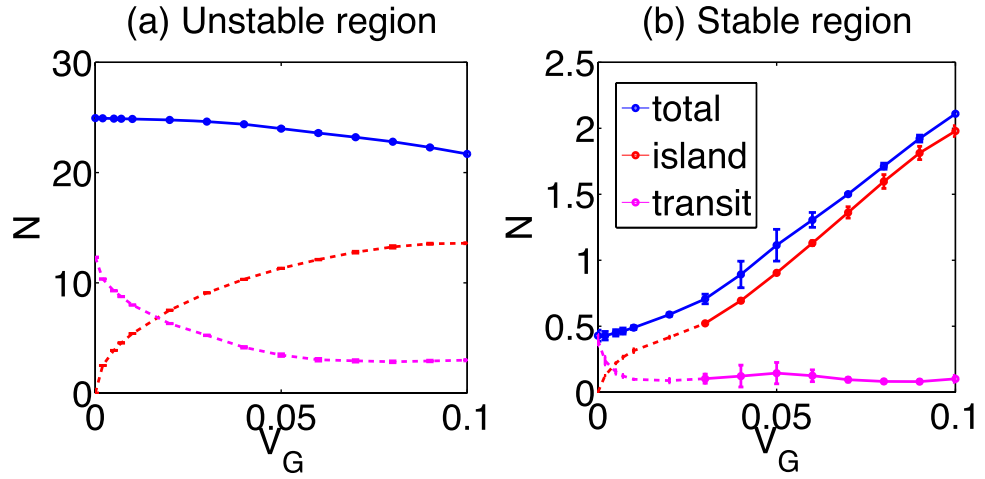


Figure 4. Amplitude dependence of the turbulence intensity at (a) $x=0$ (unstable region) and (b) $x=27$ (stable region). The blue, red and magenta lines indicate the total turbulence intensity, that inside the trapped region, and that outside the trapped region, respectively.

$$V_G > \left(\frac{\pi\omega_G}{q_x\Delta} \right)^2 \frac{(1+k_y^2)^2}{2k_y^2q_x^2}. \quad (10)$$

When both conditions, Eqs (9) and (10), are satisfied, the trapped loss is important even when the curvature of the EGAM is smaller than that of the mean flow. Substituting the simulation parameters, the overall condition is $V_G > 0.02$, which is consistent with the simulation results. Actually, the curvature of the EGAM is always smaller than that of the mean flow in the present simulation, $V_G < (q_x\Delta)^{-2}V_{MF}$. If $V_G < (q_x\Delta)^{-2}V_{MF}$ is satisfied, the curvature of the mean flow is completely suppressed by the EGAM, depending on the phase, and even the turbulence which corresponds to the transit QPs can leak into the stable region with the EGAM frequency.

We study the dependence of the turbulence intensity $N = \int_{x-\pi q_x^{-1}}^{x+\pi q_x^{-1}} dx \int dk_x N_k$ in the unstable and stable regions on the amplitude of the EGAM. Figure 4(a) illustrates the dependence of the turbulence intensity at $x=0$ (the unstable region) on the EGAM amplitude. The intensity N is calculated from the ensemble average, and the error bar is estimated from the standard deviation. The intensity N , which is calculated from the whole region in k_x -space, decreases with V_G , whose amplitude dependence is fitted to V_G^{-2} . The amplitude dependence in the stable region, $x=27$, is shown in Fig. 4(b). The turbulence intensity increases with V_G , which clearly shows that the EGAM can enhance turbulence. The total N in the stable region scales as $N = \alpha V_G^{1.5} + N_{transit}$, where the first term corresponds to the trapped loss, α is a constant parameter, $\alpha \approx 50$, and $N_{transit}$ is the component of the transit loss. Within the hypothesis that the trapped loss is perturbatively added to the transit loss, this parameter dependence can be understood: the intensity of the trapped turbulence is proportional to V_G and the spectral width increases with $k_{sep} \propto \sqrt{V_G}$. Their product yields the amplitude to the power 1.5.

The present mechanism of turbulence enhancement is discussed below in the contexts of experiments, and first-principle simulations. In the LHD, large amplitude EGAMs are observed with amplitude $e\phi_G/T \approx 1$. Using the experimental parameters, the condition for the trapped turbulence, Eq. (9), is estimated as $e\phi_G/T > 0.08$, so that the trapping effect of the EGAM is important. The amplitude for the trapping condition is not so large that the trapping effect could be important even for the turbulence driven GAM, whose observed amplitude is around $e\phi_G/T \sim 0.1^{27}$. In the case of the gyrokinetic simulations by Zarzoso and others^{7,8}, the shear layer is much narrower than the EGAM wavelength, $q_x\Delta < 1$, which is similar to that in this letter. Thus, the trapped turbulence could leak into the stable region. The amplitude of the EGAM is around $V_G \sim 0.1 - 1$, so the intensity of the leaked turbulence is expected to be comparable to that in the unstable region from the scaling obtained in this study. Therefore, the EGAM has a significant effect on the turbulence in the stable region, which leads to a substantial deterioration of the transport barrier as reported in the reference.

Finally, the propagation property of the trapped turbulence is compared with the other processes. The propagation characteristics are summarized in Table 1. The trapped turbulence propagates with the phase velocity of the EGAM (propagation speed is independent on the background profiles such as density and temperature gradients). The increase of the turbulence precedes the change of the background profiles. Thus, the turbulence in the stable region shows the non-Fickian transport properties. This is a new mechanism of the turbulence propagation, which is different from the ordinary turbulence spreading or avalanches^{16,18,19}. The turbulence intensity is determined by that of the trapped turbulence I_{trap} , while the theoretical expression of the turbulence intensity of the avalanche has not been reported. The radial flux of the turbulence clump by the trapped turbulence by the EGAM is $\Gamma_{EGAM} = q_x^{-1}\omega_G I_{trap}(V_G)$, and that by the turbulence spreading is $\Gamma_{spread} \sim V_d |\tilde{\phi}|^2$. The intensity of the radial flux by the EGAM can dominate that by the turbulence spreading when q_x is small, and/or the amplitude is

	propagation speed	turbulence intensity	propagation distance
avalanche ^{19,20}	$\sim V_d$	$\langle \tilde{\phi} ^2 \rangle$	$\sim a$
turbulence spreading ¹⁶	$\sim V_d$	$ \phi ^2$	$\sim 10\rho_i$
EGAM	$q_x^{-1}\omega_G$	$I_{trap}(V_G)$	$q_x^{-1}\Delta\omega^{-1}\omega_G$

Table 1. Comparison of turbulence propagation processes. Variables are shown in a dimensional form.

large. The propagation distance of the trapped turbulence is $\omega_G\Delta\omega^{-1}q_x^{-1}$, in which the turbulence decays algebraically, while the distance is around $10\rho_i$ in the case of the turbulence spreading, where the turbulence decays exponentially. Thus, the range area of the influence of the trapped turbulence can be a plasma size.

Discussion

In conclusion, two novel effects of the EGAM on turbulence are proposed by studying the phase-space dynamics of turbulence. Spatially inhomogeneous turbulence in the presence of transport barrier is considered. In the turbulence unstable region, the shear of the EGAM suppresses the turbulence. On the other hand, the turbulence trapped by EGAM leaks into the stable region across the transport barrier. Hence, turbulence is enhanced by the EGAM. The condition for the wave-trapping effect to be dominant is obtained, which is consistent with the simulations. The trapped turbulence by the EGAM can propagate independently from the gradients of density and temperature, which leads to the non-Fickian transport. Hence, there appear a new global characteristic velocity for turbulence dynamics, in addition to the local group velocity and that of the turbulence spreading. This manuscript provides a basis to consider whether a coherent wave breaks or strengthens transport barriers.

Methods

Simulation conditions. A monochromatic k_y -spectrum is assumed for simplicity²⁶, and the time evolution of N_k is calculated in the phase space of (x, k_x) . We prescribe $\gamma_L(x, k_x)$ and $V_y(x, t)$ as

$$\gamma_L(x, k_x) = \gamma_0 \exp\left(-\left|\frac{x}{\Delta x}\right|^{n_x}\right) \exp\left(-\left|\frac{k_x}{\Delta k}\right|^{n_k}\right), \quad (11)$$

$$V_y(t, x) = V_G \sin(q_x x - \omega_G t) + V_{MF} \left\{ \tanh\left[\frac{(x + x_0)}{\Delta}\right] - \tanh\left[\frac{(x - x_0)}{\Delta}\right] - 1 \right\}. \quad (12)$$

Here, V_G is a given parameter, since the EGAM survives regardless of the presence of turbulence. We implicitly assume that the scale length of the EP-density is much longer than the wavelength of the EGAM. The calculation region is $|x| < x_{max}$, $|k_x| < k_{x,max}$. Neumann type boundary conditions are chosen: the derivatives of N_k with respect to x and k_x are set to be zero at the boundaries. The simulations are performed with the set of the parameters; $x_{max} = 60, k_{x,max} = 6.0, k_y = 1, \gamma_0 = 0.01, \Delta\omega = 0.01, \Delta x = x_0 = 15, \Delta k = 1, n_r = 5, n_k = 2, q_x = 0.4, \omega_G = 0.01, V_G = 0 - 0.1, V_{MF} = 0.12, \Delta = 2$. The initial condition for N_k is given as $N_k(x, k_x, t = 0) = \gamma_L(x, k_x)/\Delta\omega$. We calculate the time evolution of N_k numerically.

References

- Diamond, P. H., Itoh, S.-I., Itoh, K. & Hahm, T. S. Zonal flows in plasma – a review. *Plasma Phys. Control. Fusion* **47**, R35 (2005).
- Busse, F. H. Convection driven zonal flows and vortices in the major planets. *Chaos* **4**, 123 (1994).
- Okamoto, T. J. *et al.* Resonant absorption of transverse oscillations and associated heating in a solar prominence. I. Observational aspects. *The Astrophysical Journal* **809**, 71 (2015).
- Hughes, D. W. *et al.* The Solar Tachocline. *Cambridge Univ. Press* (2007).
- Hallatschek, K. & Biskamp, D. Transport Control by Coherent Zonal Flows in the Core/Edge Transitional Regime. *Phys. Rev. Lett.* **86**, 1223 (2001).
- Conway, G. D. *et al.* Mean and Oscillating Plasma Flows and Turbulence Interactions across the L–H Confinement Transition. *Phys. Rev. Lett.* **106**, 065001 (2011).
- Zarzoso, D. *et al.* Impact of Energetic-Particle-Driven Geodesic Acoustic Modes on Turbulence. *Phys. Rev. Lett.* **110**, 125002 (2013).
- Dumont, R. J. *et al.* Interplay between fast ions and turbulence in magnetic fusion plasmas. *Plasma Phys. Control. Fusion* **55**, 124012 (2013).
- Jhang, H. *et al.* Impact of zonal flows on edge pedestal collapse. *Nucl. Fusion* **57**, 022006 (2017).
- Itoh, K., Hallatschek, K. & Itoh, S.-I. Coherent structure of zonal flow and onset of turbulent transport. *Plasma Phys. Control. Fusion* **47**, 451 (2005).
- Fu, G. Y. Energetic-Particle-Induced Geodesic Acoustic Mode. *Phys. Rev. Lett.* **101**, 185002 (2008).
- Ido, T. *et al.* Strong Destabilization of Stable Modes with a Half-Frequency Associated with Chirping Geodesic Acoustic Modes in the Large Helical Device. *Phys. Rev. Lett.* **116**, 015002 (2016).
- Osakabe, M. *et al.* Indication of bulk-ion heating by energetic particle driven Geodesic Acoustic Modes on LHD. *IAEA FEC EX/10-3* (2014).
- Sasaki, M. *et al.* Energy channeling from energetic particles to bulk ions via beam-driven geodesic acoustic modes—GAM channeling. *Plasma Phys. Control. Fusion* **53**, 085017 (2011).
- Kaw, P., Singh, R. & Diamond, P. H. Coherent nonlinear structures of drift wave turbulence modulated by zonal flows. *Plasma Phys. Control. Fusion* **44**, 51 (2002).
- Garbet, X. *et al.* Front propagation and critical gradient transport models. *Phys. Plasmas* **14**, 122305 (2007).
- Hahm, T. S. *et al.* On the dynamics of edge-core coupling. *Phys. Plasmas* **12**, 090903 (2005).
- Gurcan, O. D., Diamond, P. H., Hahm, T. S. & Lin, Z. Dynamics of turbulence spreading in magnetically confined plasmas. *Phys. Plasmas* **12**, 032303 (2005).
- Diamond, P. H. & Hahm, T. S. On the dynamics of turbulent transport near marginal stability. *Phys. Plasmas* **2**, 3640 (1995).

20. Sarazin, Y. *et al.* Large scale dynamics in flux driven gyrokinetic turbulence. *Nucl. Fusion* **50**, 054004 (2010).
21. Politzer, P. A. Observation of Avalanchelike Phenomena in a Magnetically Confined Plasma. *Phys. Rev. Lett.* **84**, 1192 (2000).
22. Guo, Z., Chen, L. & Zonca, F. Radial Spreading of Drift-Wave–Zonal-Flow Turbulence via Soliton Formation. *Phys. Rev. Lett.* **103**, 055002 (2009).
23. Itoh, K., Itoh, S.-I., Yagi, M. & Fukuyama, A. Seesaw Mechanism in Turbulence-Suppression by Zonal Flows. *J. Plasma Fusion Res.* **8**, 119 (2009).
24. Sasaki, M. *et al.* A branch of energetic-particle driven geodesic acoustic modes due to magnetic drift resonance. *Phys. Plasma* **23**, 102501 (2016).
25. Stix, T. H. *Waves in Plasmas*. New York: American Institute of Physics (1992).
26. Singh, R. *et al.* Coherent structures in ion temperature gradient turbulence-zonal flow. *Phys. Plasmas* **21**, 102306 (2014).
27. Ido, T. *et al.* Geodesic–acoustic-mode in JFT-2M tokamak plasmas. *Plasma Phys. Control. Fusion* **48**, S41 (2006).

Acknowledgements

This work was partly supported by a grant-in-aid for scientific research of JSPS, Japan (16K18335, 16H02442, 15H02155, 17H06089, 17K06994) and by the collaboration programs of NIFS (NIFS15KNST089, NIFS17KNST122) and of the RIAM of Kyushu University.

Author Contributions

M.S., K.I., K.H. and M.L. carried out theory and performed numerical simulations. N.K., Y.K., S.I.I. gave comments and suggestions, and all authors reviewed the manuscript.

Additional Information

Competing Interests: The authors declare that they have no competing interests.

Publisher's note: Springer Nature remains neutral with regard to jurisdictional claims in published maps and institutional affiliations.



Open Access This article is licensed under a Creative Commons Attribution 4.0 International License, which permits use, sharing, adaptation, distribution and reproduction in any medium or format, as long as you give appropriate credit to the original author(s) and the source, provide a link to the Creative Commons license, and indicate if changes were made. The images or other third party material in this article are included in the article's Creative Commons license, unless indicated otherwise in a credit line to the material. If material is not included in the article's Creative Commons license and your intended use is not permitted by statutory regulation or exceeds the permitted use, you will need to obtain permission directly from the copyright holder. To view a copy of this license, visit <http://creativecommons.org/licenses/by/4.0/>.

© The Author(s) 2017